molecules

MDPI

*Article*

# Cytoprotective Polyketides from Sponge-Derived Fungus *Lopadostoma pouzarii*

**Phan Thi Hoai Trinh [1,†], Anton N. Yurchenko [2,*,†], Olga O. Khmel [3], Trang Vo Thi Dieu [1], Ngo Thi Duy Ngoc [1], Elena V. Girich [2], Alexander S. Menshov [2], Natalya Y. Kim [2], Ekaterina A. Chingizova [2], Tran Thi Thanh Van [1], Jong Seok Lee [4], Hyi-Seung Lee [4] and Ekaterina A. Yurchenko [2,*]**

1 Nhatrang Institute of Technology Research and Application, Vietnam Academy of Science and Technology, Nha Trang 650000, Vietnam
2 G.B. Elyakov Pacific Institute of Bioorganic Chemistry, Far Eastern Branch of Russian Academy of Science, Prospect 100-Letiya Vladivostoka, 159, Vladivostok 690022, Russia
3 Institute of High Technologies and Advanced Materials, Far Eastern Federal University, 10 Ajax Bay, Russky Island, Vladivostok 690922, Russia
4 Marine Natural Products Chemistry Laboratory, Korea Institute of Ocean Science and Technology, Busan 49111, Korea
* Correspondence: yurchenkoan@piboc.dvo.ru (A.N.Y.); eyurch@piboc.dvo.ru (E.A.Y.)
† These authors contributed equally to this work.

**Abstract:** The new polyketides lopouzanones A and B, as well as the new 1-*O*-acetyl and 2-*O*-acetyl derivatives of dendrodochol B, were isolated from the sponge-derived marine fungus *Lopadostoma pouzarii* strain 168CLC-57.3. Moreover, six known polyketides, gliorosein, balticolid, dendrodolide G, dihydroisocoumarine, (–)-5-methylmellein, and dendrodochol B, were identified. The structures of the isolated compounds were determined by a combination of NMR and ESIMS techniques. The absolute configurations of the lopouzanones A and B were determined using the Mosher's method. The cytotoxicity of the isolated compounds against human prostate cancer cells PC-3 and normal rat cardiomyocytes H9c2 was investigated. Gliorosein showed weak DPPH radical-scavenging activity and in vitro cardioprotective effects toward rotenone toxicity and $CoCl_2$-mimic hypoxia.

**Keywords:** marine fungi; *Lopadostoma pouzarii*; sea sponge; secondary metabolites; polyketides; cytotoxicity; cardioprotection

check for updates

**Citation:** Trinh, P.T.H.; Yurchenko, A.N.; Khmel, O.O.; Dieu, T.V.T.; Ngoc, N.T.D.; Girich, E.V.; Menshov, A.S.; Kim, N.Y.; Chingizova, E.A.; Van, T.T.T.; et al. Cytoprotective Polyketides from Sponge-Derived Fungus *Lopadostoma pouzarii*. *Molecules* **2022**, *27*, 7650. https://doi.org/10.3390/molecules27217650

Academic Editor: Béla Juhász

Received: 4 October 2022
Accepted: 3 November 2022
Published: 7 November 2022

**Publisher's Note:** MDPI stays neutral with regard to jurisdictional claims in published maps and institutional affiliations.

**Copyright:** © 2022 by the authors. Licensee MDPI, Basel, Switzerland. This article is an open access article distributed under the terms and conditions of the Creative Commons Attribution (CC BY) license (https://creativecommons.org/licenses/by/4.0/).

## 1. Introduction

The marine fungi associated with marine invertebrates, especially sponges, along with the fungi of marine sediments and marine plants, are the main producers of new biologically active compounds [1].

From 1998 to 2017, fungi were found to be an important component of sponge-derived microbes—up to 73%, while actinomycetes and bacteria account for 16% and 11% of sponge-derived microbes [2]. Additionally, nearly a fifth of all new compounds from marine fungi were isolated from sponge-associated ones from 2010 to 2020 [1,3–5].

The association between sponges and fungi is very interesting for study because the level of relationship between these two groups of organisms is not entirely clear [6]. Perhaps the sponge and its associated fungi are linked by symbiosis, or there is a different type of interaction. Sponges have been studied for a long time as a source of cytotoxic substances [7]. However, several cases are known where the substances isolated from a sponge were then found in the microbials isolated from this sponge. For instance, antimalarial alkaloid manzamine A, isolated from a marine sponge *Acanthostrongylophora* aff. *ingens* [8], was later isolated from its symbiont *Micromonospora* sp. [9]. 1,2-Bis(1H-indol-3-yl) ethane-1,2-dione, an indole alkaloid from the marine sponge *Smenospongia* sp. [10], was later isolated from marine fungus *Penicillium vinaceum*, associated with marine sponge *Hyrtios erectus* [11].

The *Lopadostoma pouzarii* fungus was first isolated from the *Fraxini excelsioris* tree and identified as a new species in the *Lopadostoma* genus (Xylariaceae, Xylariales) [12]. Later two cultures of this fungus were sequenced and found not to belong to *Lopadostoma*, but they perhaps belong to another genus in the family Xylariaceae, probably *Whalleya* [13]. Nonetheless, both the *Lopadostoma* and the *Whalleya* genera have apparently not been studied much in terms of their secondary metabolites [14]. Only antimicrobial azaphilone pigments sassafrins A-D were isolated from another *Lopadostomaceae* fungus *Creosphaeria sassafras* [15]. Other Xylariales fungi are more studied and produced most of the various polyketides [14].

In the continuation of our investigation of the biodiversity and secondary metabolites of Vietnamese marine fungi [16,17], the *Lopadostoma pouzarii* strain 168CLC-57.3 was isolated from an unidentified marine sponge and cultured for low-molecular weight metabolite isolation.

Herein, we report the isolation, structure elucidation, and biological activity of ten compounds, including four new ones (Figure 1) from the marine sponge-derived fungus *L. pouzarii*.

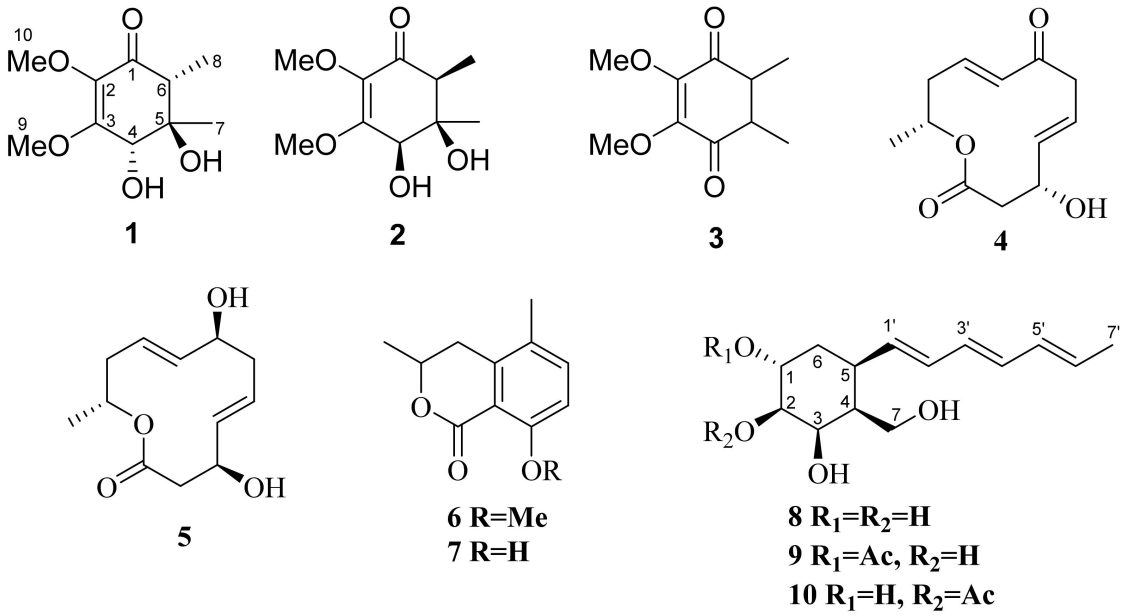



**Figure 1.** Structures of isolated compounds **1–10**.

## 2. Results

### *2.1. Isolation and Identification of Compounds* **1–10**

The molecular formula of compound **1** was determined as $C_{10}H_{16}O_5$, based on the HRESIMS data (*m/z* 239.0890 $[M+Na]^+$) corresponding with the $^{13}C$ NMR data. An analysis of $^1H$ and $^{13}C$ NMR data (Table 1, Figures S1–S5 from Supplementary Materials) of **1** using DEPT and HSQC techniques revealed the presence of two methoxy-($\delta_C$ 57.6, $\delta_H$ 3.92; $\delta_C$ 59.3, $\delta_H$ 3.47), two methyl ($\delta_C$ 12.9, $\delta_H$ 1.08; $\delta_C$ 20.6, $\delta_H$ 1.11), and two methine ($\delta_C$ 72.9, $\delta_H$ 4.14; $\delta_C$ 51.4, $\delta_H$ 2.25) groups, as well as a quaternary $sp^3$-carbon ($\delta_C$ 72.8) and three quaternary $sp^2$-carbons ($\delta_C$ 196.4; $\delta_C$ 160.6; $\delta_C$ 134.7), chemical shifts of which represented a typical case of α,β-unsaturated ketone. In addition, there were two hydroxyl protons ($\delta_H$ 4.76, $\delta_H$ 5.74) in the structure.

**Table 1.** NMR data (700 MHz, DMSO-$d_6$, $\delta$ in ppm) for compounds **1** and **2**.

| Position | 1 | | 2 | |
|---|---|---|---|---|
| | $\delta_C$, mult | $\delta_H$ (*J* in Hz) | $\delta_C$, mult | $\delta_H$ (*J* in Hz) |
| 1 | 196.4, C | | 194.9, C | |
| 2 | 134.7, C | | 135.8, C | |
| 3 | 160.6, C | | 159.5, C | |
| 4 | 72.9, CH | 4.14, d (6.4) | 71.9, CH | 4.25, d (7.4) |
| 5 | 72.8, C | | 73.7, C | |
| 6 | 51.4, CH | 2.20, q (7.4) | 49.1, CH | 2.30, q (6.9) |
| 7 | 20.6, $CH_3$ | 1.11, s | 24.1, $CH_3$ | 1.19, s |
| 8 | 12.9, $CH_3$ | 1.08, d (7.4) | 8.6, $CH_3$ | 1.05, d (6.9) |
| 9 | 57.6, $CH_3$ | 3.92, brs | 58.4, $CH_3$ | 3.93, s |
| 10 | 59.3, $CH_3$ | 3.47, brs | 59.4, $CH_3$ | 3.48, s |
| 4-OH | | 5.74, d (6.4) | | 5.32, d (7.4) |
| 5-OH | | 4.76, brs | | 4.26, s |

The HMBC correlations (Figure 2 and Figure S4 from Supplementary Materials) from H-6 ($\delta_H$ 2.25) to C-1 ($\delta_C$ 196.4) and C-5 ($\delta_C$ 72.8), as well as from H-4 ($\delta_C$ 4.14) to C-2 ($\delta_C$ 134.7), C-3 ($\delta_C$ 160.6), and C-5 showed a structure of a cyclohexenone ring in **1**. The locations of the methyl groups at C-5 ($\delta_C$ 72.8) and C-6 ($\delta_C$ 51.4), the methoxyl groups at C-2 ($\delta_C$ 134.7) and C-3 ($\delta_C$ 160.6), and the hydroxyl groups at C-4 ($\delta_C$ 72.9) and C-5 were determined by HMBC correlations from $C_3$-7 ($\delta_H$ 1.11) to C-5, from $C_3$-8 ($\delta_H$ 1.08) to C-6, from $C_3$-9 ($\delta_H$ 3.92) to C-3, from $C_3$-10 ($\delta_H$ 3.47) to C-2, from 4-O<u>H</u> ($\delta_C$ 5.74) to C-3 and C-4, and from 5-O<u>H</u> ($\delta_C$ 4.76) to C-5 and C-7 ($\delta_C$ 20.6).

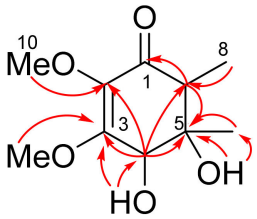
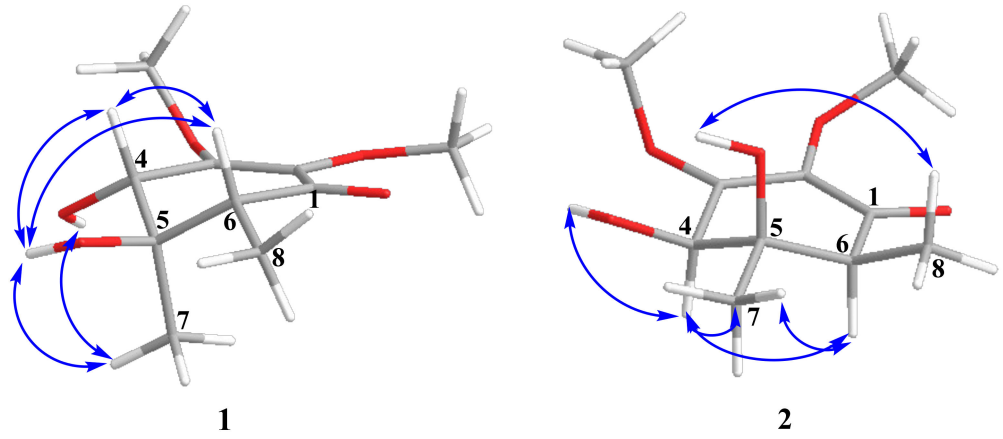



**Figure 2.** Key HMBC correlations in lopouzanone A (**1**).

The relative configurations of **1** were assigned based on ROESY correlations (Figure 3 and Figure S6 from Supplementary Materials) between H-4 ($\delta_H$ 4.14), H-6 ($\delta_H$ 2.20), and 5-O<u>H</u> ($\delta_H$ 4.76) and between $H_3$-7 and 4-O<u>H</u>. The absolute configuration of **1** was established by the modified Mosher's method [18]. The esterification of **1** with (*S*)- and (*R*)-MTPA chloride occurred at the C-4 hydroxy group to yield the (*R*)-and (*S*)-MTPA esters **1a** and **1b**, respectively. The observed chemical shift differences $\Delta\delta(\delta_S\text{-}\delta_R)$ (Figure 4 and Figures S8–S11 from Supplementary Materials) indicated the 4*S* configuration, and therefore, the absolute configurations of **1** were established as 4*S*,5*R*,6*R*. Compound **1** was named lopouzanone A.

The molecular formula of compound **2** was determined as $C_{10}H_{16}O_5$ (same as **1**), based on the HRESIMS data (*m*/*z* 239.0889 $[M+Na]^+$) corresponding with the $^{13}C$ NMR data. An analysis of the NMR data of **2** (Table 1, Figures S12–S16 from Supplementary Materials) and a comparison them with those for lopouzanone A (**1**) showed the chemical shift differences, especially in the chiral part of the molecule. On the other hand, the HMBC correlations of **2** (Figure S15 from Supplementary Materials) were in complete agreement with those for **1**, which proved the same planar structure.




**1** **2**

**Figure 3.** Key ROESY correlations in compounds **1** and **2**.

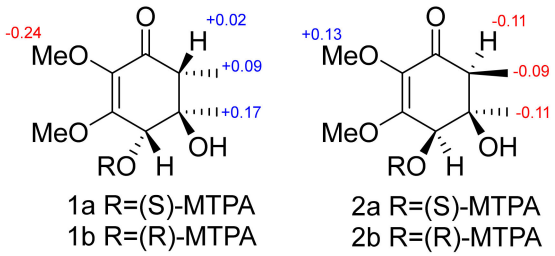



**Figure 4.** $\Delta\delta(\delta_S\text{-}\delta_R)$ values (in ppm) for MTPA esters of **1** and **2**.

The relative configurations of **2** were assigned based on the ROESY correlations (Figure 3 and Figure S17 from Supplementary Materials) between H-4 ($\delta_H$ 4.25), H-6 ($\delta_H$ 2.32), and $H_3$-7 ($\delta_H$ 1.19). The absolute configuration of **2** was established by the modified Mosher's method [18]. The esterification of **2** with (*S*)- and (*R*)-MTPA chloride occurred at the C-4 hydroxy group to yield the (*R*)-and (*S*)-MTPA esters **2a** and **2b**, respectively. The observed chemical shift differences $\Delta\delta(\delta_S\text{-}\delta_R)$ (Figure 4) indicated the 4*R* configuration, and therefore, the absolute configurations of **2** were established as 4*R*,5*R*,6*S*. Compound **2** was named lopouzanone B.

The molecular formulas of compounds **9** and **10** were determined as $C_{16}H_{24}O_5$ on the basis of the HRESIMS data (*m*/*z* 319.1516 $[M+Na]^+$) and confirmed by the $^{13}C$ NMR data. The NMR data of **9** were very close to those for the known dendrodochol B (**8**) [19], with the exception of the proton and carbon signals of the methines at C-1 and C-2 and the methylene at C-6 (Table 2, Figures S34–S40 from Supplementary Materials). These changes, the characteristic signals of the acetate group ($\delta_C$ 172.9, 21.2; $\delta_H$ 2.05), and the molecular mass difference (42 mass units) between **8** and **9** suggested the acetylation of the hydroxy-group at C-1. This was proved by HMBC (Figure S39 from Supplementary Materials) from H-1 ($\delta_H$ 3.79) to C-8 ($\delta_C$ 172.9). The NMR spectra of compound **10** (Table 2, Figures S42–S45 from Supplementary Materials) suggested the presence of an acetate group at C-2, which was proved by HMBC from H-2 to C-8. Thus, compounds **9** and **10** were named 1-*O*-acetyl dendrodochol B and 2-*O*-acetyl dendrodochol B, respectively. An analysis of the vicinal constants for compounds **8**, **9,** and **10** revealed the same relative configurations of all stereocenters. Moreover, the absolute stereochemistry of **9** and **10** was assumed to be the same as previously described for dendrodochol B (**8**) (1*R*,2*S*,3*R*,4*S*,5*R*) based on their obvious biosynthetic relationship.

**Table 2.** NMR data (600 MHz, methanol-$d_4$, $\delta$ in ppm) for compounds **8–10**.

| Position | 8 | | 9 | | 10 | |
|---|---|---|---|---|---|---|
| | $\delta_C$, mult | $\delta_H$ (J in Hz) | $\delta_C$, mult | $\delta_H$ (J in Hz) | $\delta_C$, mult | $\delta_H$ (J в Гц) |
| 1 | 70.3, CH | 3.79, ddd (12.5, 11.2, 4.7) | 74.1, CH | 5.05, ddd (12.0, 10.0, 4.9) | 67.6, CH | 4.02, ddd (11.7, 10.0, 4.9) |
| 2 | 78.4, CH | 3.24, dd (9.4; 2.8) | 75.5, CH | 3.49, dd (9.8, 2.8) | 81.1, CH | 4.53, dd (9.9, 2.7) |
| 3 | 71.7, CH | 4.15, t (2.4) | 71.6, CH | 4.20, t (2.8) | 68.9, CH | 4.27, t (2.7) |
| 4 | 48.3, CH | 1.42, m | 48.1, CH | 1.45, m | 48.0, CH | 1.49, m |
| 5 | 37.5, CH | 2.36, tdd (12.5, 9.4, 4.0) | 37.2, CH | 2.40, tdd (12.5, 9.0, 4.2) | 37.2, CH | 2.36, tdd (12.5, 9.4, 4.0) |
| 6 | 40.9, $CH_2$ | 1.83, ddd (12.5, 4.7, 4.0) 1.25, q (12.5) | 37.6, $CH_2$ | a: 1.89, dt (12.5, 4.5) b: 1.29, q (12.5) | 40.9, $CH_2$ | a: 1.91, ddd (12.5, 4.9, 4.0) b: 1.33, q (12.5) |
| 7 | 62.4, $CH_2$ | 3.57, d (6.5) | 62.2, $CH_2$ | 3.59, m | 62.0, $CH_2$ | 3.55, m |
| 8 | | | 172.9, C | | 172.8, C | |
| 9 | | | 21.2, $CH_3$ | 2.05, s | 21.1, $CH_3$ | 2.12, s |
| 1′ | 137.0, CH | 5.43, dd (14.2, 9.0) | 136.2, CH | 5.42, dd (14.1, 9.0) | 136.4, CH | 5.44, dd (14.1, 9.0) |
| 2′ | 131.3, CH | 6.03–6.13, m | 131.1, CH | 6.05–6.13, m | 131.1, CH | 6.05–6.13, m |
| 3′ | 133.1, CH | 6.03–6.13, m | 133.1, CH | 6.05–6.13, m | 133.1, CH | 6.05–6.13, m |
| 4′ | 132.9, CH | 6.03–6.13, m | 133.0, CH | 6.05–6.13, m | 133.0, CH | 6.05–6.13, m |
| 5′ | 132.3, CH | 6.03–6.13, m | 132.7, CH | 6.05–6.13, m | 132.5, CH | 6.05–6.13, m |
| 6′ | 129.9, CH | 5.68, dq (14.2, 6.9) | 130.0, CH | 5.69, dq (14.2, 6.9) | 130.0, CH | 5.68, dq (14.1, 6.9) |
| 7′ | 18.3, $CH_3$ | 1.75, d (6.9) | 18.3, $CH_3$ | 1.75, d (6.9) | 18.3, $CH_3$ | 1.75, d (6.8) |

In addition to the new compounds **1**, **2**, **9,** and **10**, six known polyketides were isolated from this fungal strain: gliorosein (**3**) [20], balticolid (**4**) [21], dendrodolide G (**5**) [22], dihydroisocoumarine (**6**) [23], (–)-5-methylmellein (**7**) [24], and dendrodochol B (**8**) [19].

### *2.2. Biological Activity of Isolated Compounds*

Compounds **6** and **7** were isolated in an insufficient amount; so, their biological activity was not estimated. The radical-scavenging activity of compounds **1–5**, **8**, and **9** was determined by DPPH assay (Table 3). Gliorosein (**3**) showed a statistically significant DPPH-radical scavenging activity and decreased the amount of DPPH radical by 13.9% at a concentration of 100 μM.

**Table 3.** DPPH radical scavenging and cytotoxic activities of compounds **1–5**, **8**, and **9**.

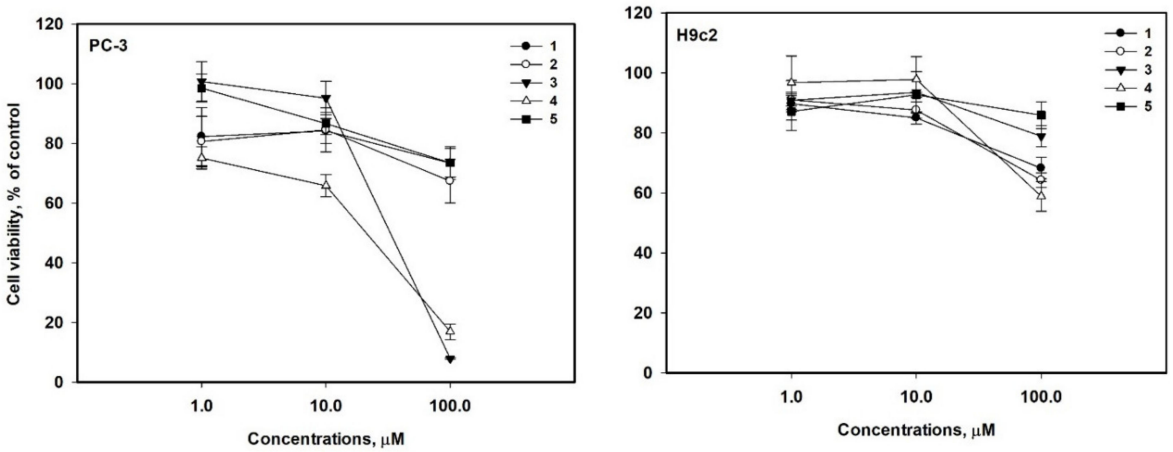
| Compound | DPPH Radicals, % of Control [1] | $IC_{50}$, μM | |
|---|---|---|---|
| | | PC-3 | H9c2 |
| **1** | 93.8 ± 0.5 | >100 | >100 |
| **2** | 100.2 ± 1.0 | >100 | >100 |
| **3** | 86.1 ± 1.8 * | 58.9 ± 1.5 | >100 |
| **4** | 98.6 ± 3.4 | 38.9 ± 1.9 | >100 |
| **5** | 98.9 ± 1.4 | >100 | >100 |
| **8** | 99.4 ± 3.3 | >100 | >100 |
| **9** | 102.7 ± 1.8 | >100 | >100 |
| Ascorbic acid | 10.5 ± 3.2 | | |

* The differences between this and the control are significant with $p \leq 0.05$. [1] The effect of compounds at a concentration of 100 μM.

The cytotoxic activity of compounds **1–5**, **8**, and **9** toward human prostate cancer PC-3 cells and the rat normal cardiomyocytes H9c2 line is presented in Table 3. The investigated compounds showed a moderate or weak cytotoxic activity. All the compounds at a concentration of 100 μM showed the same cytotoxicity for the rat normal cardiomyocytes H9c2, and none of them decreased H9c2 cell viability by more than by 42%. At a concentration of 10 μM, all the compounds decreased the H9c2 viability by 3–15%. The compounds **1**, **2**, **5**, **8**, and **9** showed a weak cytotoxic activity toward the human prostate cancer PC-3 cells. They decreased the PC-3 cell viability by only 27–32% at a concentration of 100 μM; so, its

concentrations of 50% inhibition were not calculated. The compounds **3** and **4** were more toxic for PC-3 cells, with the $IC_{50}$ of 58.9 μM and 38.9 μM, respectively.

The cytotoxic activity of compounds **1–5** at different concentrations is presented in Figure 5.




(**a**) (**b**)

**Figure 5.** Cytotoxic activity of compounds **1–5** at different concentrations toward PC-3 (**a**) and H9c2 (**b**) cells.

The cardioprotective effects of the isolated compounds against rotenone and cobalt chloride (II) were investigated. The influence of compound **3** at a nontoxic concentration of 10 μM on the viability of rotenone- and $CoCl_2$-treated cardiomyocytes H9c2 is presented in Figure 6. The treatment of H9c2 cells with $CoCl_2$ decreased the viability of H9c2 cells by 54.1%. Compound **3** at 10 μM increased the viability of $CoCl_2$-treated H9c2 cells by 23.5%.

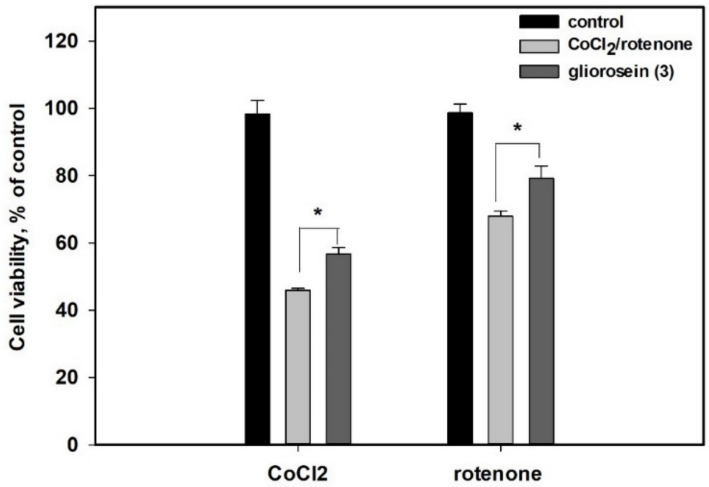



**Figure 6.** The cytoprotective activity of gliorosein (**3**) at 10 μM against $CoCl_2$-mimic hypoxia and rotenone toxicity in H9c2 cells. The data are presented as a mean ± standard error of mean (SEM). * The differences are significant with $p \leq 0.05$.

The treatment of H9c2 cells with rotenone decreased the viability of H9c2 cells by 32.1%. Compound **3** at a same concentration increased the viability of the rotenone-treated H9c2 cells by 16.6%. Both of these results were statistically significant. Other isolated compounds were not effective in the experiments.

## 3. Discussion

So, ten polyketides were isolated from the *Lopadostoma pouzarii* fungus, which was isolated from the marine environment for the first time. Known gliorosein (**3**) was reported earlier only from terrestrial fungi *Gliocladium* spp. [25].

The biosynthesis of isolated new compounds was suggested (Figure 7). We supposed that the biogenesis of lopouzanones A and B was very probably related with gliorosein (**3**). As was investigated earlier [26], gliorosein originates from tetraketyde 5-methylorsellinic acid. A hydroxylation of the C-5 atom of gliorosein (**3**) gives lopouzanone B (**2**), and the reduction and hydroxylation of the direct precursor of gliorosein gives lopouzanone A (**1**). Dendrodochol B (**8**) and its derivatives **9** and **10** obviously originate from the heptaketyde precursor that cyclizes to acyl orsellinic acid, the main structural features of which are in structures of **8**–**10**. The consistent reduction, hydroxylation, side chain dihydroxylation, and stereoselective reduction of the aromatic ring yield dendrodochol B and its acetylated derivatives.

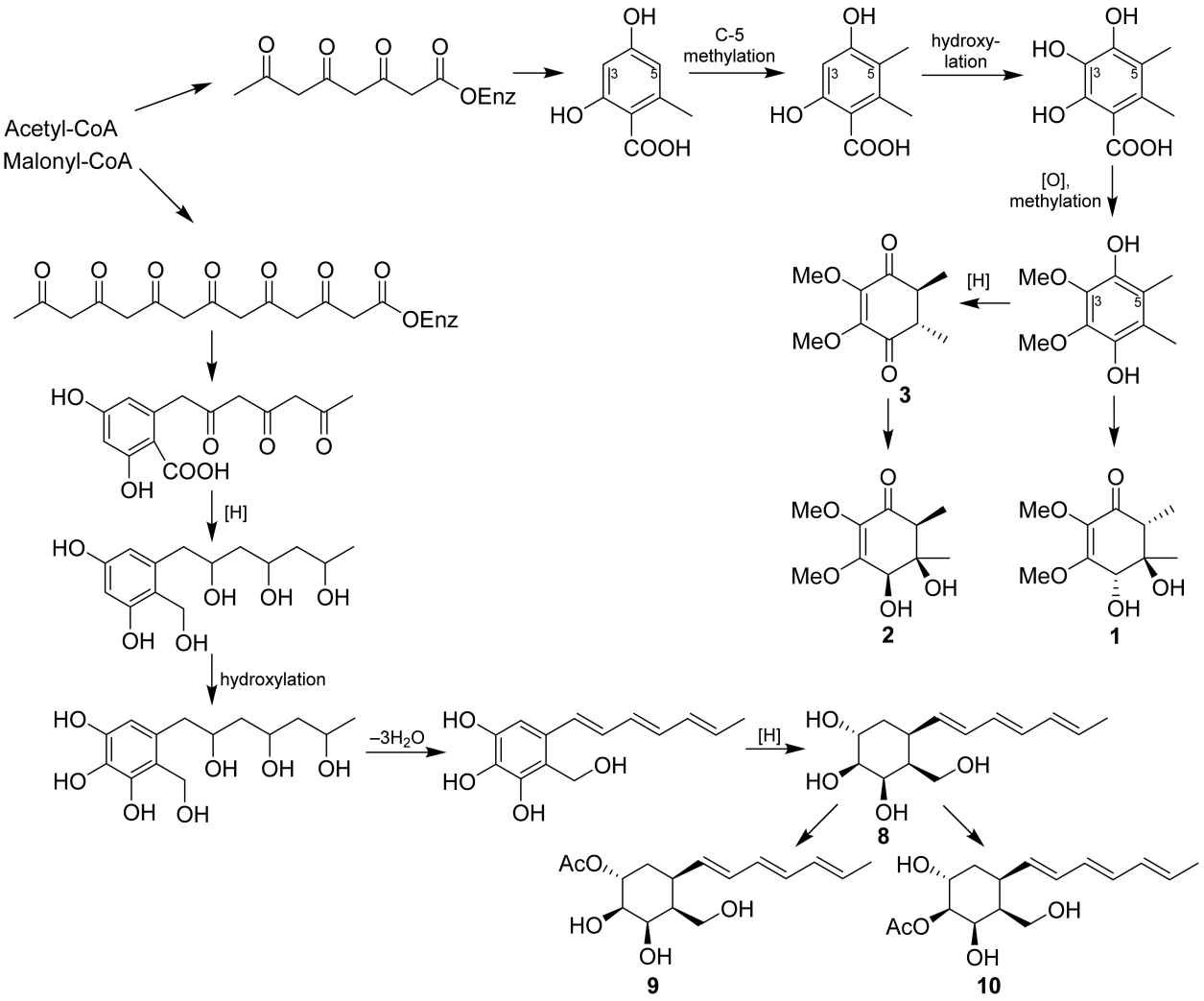



**Figure 7.** Proposal biosynthetic pathway for compounds **1**–**3** and **8**–**10**.

This is the first report about the selective cytotoxic activity of gliorosein (**3**) and balticolide (**4**) against the human prostate cancer PC-3 cells. Earlier, gliorosein was reported to be an antimicrobial compound [27], and selective cytotoxic activity against the HCT116 cell line was reported for the closely related macrolides balticolide [21] and dendrodolide E [22].

At a nontoxic concentration, gliorosein (**3**) showed cardioprotective activity against the rotenone- and $CoCl_2$-induced damage of the cardiomyocytes H9c2.

The treatment of cultured cells with $CoCl_2$ is well known and widely used in the in vitro model of hypoxia [28]. Hypoxia causes various pathological processes in the cells, including oxidative stress via the blocking of the mitochondrial respiratory chain, which results in an increase in the reactive oxygen species levels into cells [29]. $CoCl_2$ also induces oxidative stress into H9c2 cardiomyocytes via ROS formation [30]. The natural isoflavonoid rotenone used for the in vitro and in vivo modeling of Parkinson's disease inhibits the mitochondrial complex I, resulting in oxidative stress and cell damage [31]. The inhibition of mitochondrial complex I in H9c2 cardiomyocytes also alters their pro/antioxidant system balance and cell viability [32].

The antioxidant defense against oxidative stress in fungi as well as other eukaryotes is a network of enzymatic superoxide dismutase, catalases, and the thioredoxin system. The fungal response to oxidative stress is therefore complex and necessitates the collaborative involvement of cognate regulators such as the HOG pathway, Yap1, and Skn7 [33]. Nonenzymatic radical-scavenging secondary metabolites have overlapping roles in intercepting ROS and in turning over the cellular buffer of reductants. Polyketides are one of these radical-scavenging compounds. Gliorosein (**3**) showed a weak radical-scavenging activity in a cell-free assay and can protect H9c2 cells from rotenone- and hypoxia-induced death via ROS scavenging. The anti-radical effect of gliorosein (**3**) in the DPPH test was not very high, but it was statistically significant. This effect is difficult to correlate directly with its intracellular action on ROS since the difference in the concentration of free radicals in the cell and in the DPPH test can be significant. Earlier, we observed how other orsellinic acid derivatives showed a weak activity in the DPPH test and were effective in a cellular model of Parkinson's disease and were also associated with oxidative stress and ROS [34]. Nevertheless, the cardioprotective properties of gliorosein (**3**) in hypoxia conditions need future investigations.

## 4. Materials and Methods

### *4.1. General*

Optical rotations were measured on a Perkin-Elmer 343 polarimeter (Perkin Elmer, Waltham, MA, USA). UV spectra were recorded on a Shimadzu UV-1601PC spectrometer (Shimadzu Corporation, Kyoto, Japan) in methanol. CD spectra were measured with a Chirascan-Plus CD spectrometer (Leatherhead, UK) in methanol. NMR spectra were recorded on Bruker DPX-300, Bruker DPX-500, Bruker DPX-600, and Bruker DRX-700 spectrometers (Bruker BioSpin GmbH, Rheinstetten, Germany), using TMS as an internal standard. Low-pressure liquid column chromatography was performed using ODS gel (12 nm, S-75 μM, YMC CO., Kyoto, Japan). HRESIMS spectra were measured on a Maxis Impact mass spectrometer (Bruker Daltonics GmbH, Rheinstetten, Germany).

Low-pressure liquid column chromatography was performed using silica gel (50/100 μm, Imid Ltd., Krasnodar, Russia). Plates precoated with silica gel (5–17 μm, 10 cm × 10 cm, Imid Ltd., Krasnodar, Russia), and 60 RP-18 $F_{254}S$ silica gel (20 cm × 20 cm, Merck KGaA, Darmstadt, Germany) was used for thin-layer chromatography. Preparative HPLC was carried out on an HPLC system consisting of a PrimeLine Binary pump (Analytical Scientific Instruments, Inc., El Sobrante, CA, USA) with a RI-101 refractometer (Shoko Scientific Co. Ltd., Yokohama, Japan) and a Shimadzu LC-20 chromatograph (Shimadzu USA Manufacturing, Canby, OR, USA) with a Shimadzu RID-20A refractometer (Shimadzu Corporation, Kyoto, Japan) using the semi-preparative columns YMC-Pack-ODS-A, 250 × 10 mm, 5 μm) (YMC Corporation, Kyoto, Japan) and YMC ODS-AM (YMC Co., Ishikawa, Japan) (5 μm, 10 mm × 250 mm) and YMC SIL (YMC Co., Ishikawa, Japan) (5 μm, 10 mm × 250 mm) columns.

### *4.2. Fungal Material and Fermentation*

The fungal strain 168CLC-57.3 was isolated from an unidentified sponge sample collected at Cu Lao Cham Island, Quang Nam, Vietnam. The fungus was identified as *Lopadostoma pouzarii* by gene sequence analysis of the ITS region. According to BLAST analysis, this fungus had the highest similarity to the *L. pouzarii* strain LPO (89.88%, GenBank

accession number KC774601). The strain is currently stored in the NITRA Collection of Marine Microorganisms of the Nhatrang Institute of Technology Research and Application, Vietnam, under code 168CLC-57.3 (GenBank accession number MH752441).

The fungus was cultured in 80 × 500 mL Erlenmeyer flasks, each containing rice (20.0 g), yeast extract (20.0 mg), $KH_2PO_4$ (10 mg), and natural seawater from the Nha Trang Bay (40 mL) at 28 °C for three weeks.

### *4.3. Extraction and Isolation*

The fungal mycelia and medium were extracted with EtOAc (24.0 L) and then evaporated in vacuo to yield a crude extract (6.0 g). The crude extract was separated on C18-reversed-phase silica gel (ODS) by flash column chromatography using a gradient of MeOH/$H_2O$ (1:4 to 100% MeOH, each fraction 500 mL) to yield seven fractions. The fraction eluted with 40% MeOH was purified with a semi-preparative reversed-phase HPLC (3.0 mL/min, RI detector, 10% MeOH/$H_2O$) to obtain **1** (7.6 mg, $t_R$ = 18 min), **2** (4.8 mg, $t_R$ = 32 min), and **3** (3.4 mg, $t_R$ = 7 min). Compound **4** (3.8 mg, $t_R$ = 24 min) and **5** (1.8 mg $t_R$ = 42 min) were purified from the fraction eluted with 60% MeOH through a semi-preparative reversed-phase HPLC (3.0 mL/min, RI detector, 30% MeOH/$H_2O$). The fraction eluted with 70% MeOH was separated by a semi-preparative reversed-phase HPLC (3.0 mL/min, RI detector) using an isocratic elution with 35% MeOH in $H_2O$ to yield **6** (1.3 mg). Compounds **8** (8.2 mg, $t_R$ = 34 min) and **9** (2.9 mg, $t_R$ = 42 min) were isolated from the fraction MeOH–$H_2O$ (80:20) by a semi-preparative reversed-phase HPLC (45% MeOH/$H_2O$, 3.0 mL/min). The fraction eluted with 90% MeOH was purified by HPLC on a YMC-Pack-ODS-A column eluting with MeOH–$H_2O$ (55:45) to obtain **7** (12.0 mg, $t_R$ = 26 min) and **10** (4.1 mg, $t_R$ = 43 min).

### *4.4. Isolated Compounds*

Lopouzanone A (**1**): amorphous solid; $[\alpha]_D^{20}$ − 59.3 (c 0.03, MeOH); CD (c 0.51, MeOH), $\lambda_{max}$ ($\Delta\varepsilon$) 207 (3.24), 266 (−2.32), 316 (–1.05) nm, (Figure S7 from Supplementary Materials); UV (MeOH) $\lambda_{max}$ (log $\varepsilon$) 298 (3.88), 198 (4.17), 238 (3.44) nm; $^1$H and $^{13}$C NMR data, see Table 1, (Figures S1–S6 from Supplementary Materials); HRESIMS *m*/*z* 239.0890 $[M + Na]^+$ (calcd. for $C_{10}H_{16}O_5Na$, 239.0890, Δ 0 ppm).

Lopouzanone B (**2**): amorphous solid; $[\alpha]_D^{20}$ +164.95 (c 0.097, MeOH); CD (c 0.83, MeOH), $\lambda_{max}$ ($\Delta\varepsilon$) 203 (−3.75), 262 (−2.20), 306 (3.23) nm, (Figure S18 from Supplementary Materials); UV (MeOH) $\lambda_{max}$ (log $\varepsilon$) 266 (4.06), 195 (3.71), 226 (3.25) nm; $^1$H and $^{13}$C NMR data, see Table 1, (Figures S12–S17 from Supplementary Materials); HRESIMS *m*/*z* 239.0889 $[M + Na]^+$ (calcd. for $C_{10}H_{16}O_5Na$, 239.0890, Δ 0.42 ppm).

1-*O*-acetyl dendrodochol B (**9**): amorphous solid; $[\alpha]_D^{20}$ +130.0 (c 0.01, MeOH); CD (c 0.34, MeOH), $\lambda_{max}$ ($\Delta\varepsilon$) 212 (−1.16), 219 (−1.26), 255 (−0.30), 283 (−0.25) nm, (Figure S41 from Supplementary Materials); UV (MeOH) $\lambda_{max}$ (log $\varepsilon$) 270 (3.52), 234 (3.99), 198 (3.75), 260 (3.50), 207 (3.72) nm; $^1$H and $^{13}$C NMR data, see Table 2, (Figures S36–S40 from Supplementary Materials); HRESIMS *m*/*z* 319.1516 $[M + Na]^+$ (calcd. for $C_{16}H_{24}O_5Na$, 319.1516, Δ 0.0 ppm).

2-*O*-acetyl dendrodochol B (**10**): amorphous solid; $[\alpha]_D^{20}$ +120.1 (c 0.01, MeOH); $^1$H and $^{13}$C NMR data, see Table 2, (Figures S42–S45 from Supplementary Materials); HRESIMS *m*/*z* 319.1515 $[M + Na]^+$ (calcd. for $C_{16}H_{24}O_5Na$, 319.1516, Δ 0.31 ppm).

### *4.5. DPPH Scavenging Assay*

The compounds were dissolved in DMSO, and the solutions (120 µL) were dispensed into wells of a 96-well microplate. In all, 30 µL of the DPPH (Sigma-Aldrich, Steinheim, Germany) solution in MeOH ($1.5 \times 10^{-4}$ M) was added to each well. The concentrations of the compounds in mixture were 10 and 100 µM. Pure DMSO was used as a control. The ascorbic acid was used as a positive control. The mixture was shaken and left to stand for 30 min, and the absorbance of the resulting solution was measured at 520 nm with a microplate reader MultiscanFC (ThermoLabsystems Inc., Beverly, MA, USA). The

radical scavenging activity of all compounds at 100 μM was presented as a percent of the DMSO data.

### *4.6. Bioassays*

#### 4.6.1. Cell Culture

The human cancer PC-3 cells were purchased from ATCC (Manassas, VA, USA). The rat cardiomyocytes H9c2 cells were kindly provided by Prof. Dr. Gunhild von Amsberg from Martini-Klinik Prostate Cancer Center, University Hospital Hamburg-Eppendorf, Hamburg, Germany.

#### 4.6.2. Cell Viability Assay

The PC-3 and H9c2 cells were seeded at concentrations of $5 \times 10^3$ cell/well and $3 \times 10^3$ cell/well, respectively, and the experiments were started after 24 h. The compounds at concentrations up to 100 μM were added into the wells for 48 h, and the viability of the cells was measured by an MTT (3-(4,5-dimethylthiazol-2-yl)-2,5-diphenyltetrazolium bromide) assay, which was performed according to the manufacturer's instructions (Sigma-Aldrich, Munich, Germany). All compounds were diisolved with DMSO so that the final concentration of DMSO in the cell culture was not more than 1%. Moreover, DMSO was used as a control.

The results were presented as a percent of the control data, and the concentration of the cell viability inhibition on 50% ($IC_{50}$) was calculated.

#### 4.6.3. Cardioprotective Activity of Compounds in $CoCl_2$-Mimic Hypoxia

The H9c2 cells were treated with a $dH_2O$-solution of $CoCl_2$ at a concentration of 500 μM for 2 h. Then, compounds at a concentration of 10 μM were added for 46 h. The viability of the H9c2 cells was measured by an MTT assay.

#### 4.6.4. Cardioprotective Activity of Compounds against Rotenone-Induced Toxicity

The H9c2 cells were treated with rotenone (0.1% DMSO solution) at a concentration of 10 μM for 1 h. Then, compounds at a concentration of 10 μM were added for 23 h. The viability of the H9c2 cells was measured by an MTT assay.

### *4.7. Statistical Data Evaluation*

All the data were obtained in three independent replicates, and the calculated values were expressed as mean ± standard error mean (SEM). A Student's *t*-test was performed using SigmaPlot 14.0 (Systat Software Inc., San Jose, CA, USA) to determine the statistical significance. The differences were considered statistically significant at $p < 0.05$.

## 5. Conclusions

Thus, the new polyketides lopouzanones A and B, as well as the new 1-*O*-acetyl and 2-*O*-acetyl derivatives of dendrodochol B, were isolated from the sponge-derived marine fungus *Lopadostoma pouzarii* strain 168CLC-57.3. Moreover, six known polyketides, gliorosein, balticolid, dendrodolide G, dihydroisocoumarine, (–)-5-methylmellein, and dendrodochol B, were identified. The isolated compounds showed a weak cytotoxicity against human prostate cancer cells PC-3 and normal rat cardiomyocytes H9c2. Moreover, gliorosein showed in vitro cardioprotective effects toward rotenone toxicity and $CoCl_2$-mimic hypoxia.

**Supplementary Materials:** The following supporting information can be downloaded at: https://www.mdpi.com/article/10.3390/molecules27217650/s1, Figure S7, Figure S18, Figure S25 and Figure S41: ECD spectra of compounds **1**–**3** and **9**, Figures S1–S6, S12–S17, S23, S24, S26–S40, S42–S45: NMR spectra of compounds **1**–**10**, Figures S8–S11, S19–S22: NMR spectra of MTPA-esters of compounds **1** and **2**, Figures S46–S49: HRESIMS spectra of compounds **1**, **2**, and **8**–**10**.

**Author Contributions:** Conceptualization, E.A.Y.; data curation, A.N.Y. and J.S.L.; formal analysis, A.N.Y.; funding acquisition, J.S.L.; investigation, P.T.H.T., O.O.K., T.V.T.D., N.T.D.N., E.V.G., A.S.M., N.Y.K., E.A.C., and E.A.Y.; methodology, H.-S.L.; project administration, A.N.Y. and T.T.T.V.; resources, A.N.Y., T.T.T.V. and J.S.L.; supervision, T.T.T.V. and H.-S.L.; visualization, P.T.H.T., O.O.K., E.V.G. and N.Y.K.; writing—original draft, P.T.H.T. and E.A.Y.; writing—review and editing, A.N.Y. and H.-S.L. All authors have read and agreed to the published version of the manuscript.

**Funding:** This research was funded by the Russian Foundation for Basic Research (grant number 21-53-54005 (chemical study and bioassays), the Vietnam Academy of Science and Technology (grant number VAST06.02/21-22), and the Korea Institute of Ocean Science and Technology (grant numbers PM62060 and PEA0021).

**Institutional Review Board Statement:** Not applicable.

**Informed Consent Statement:** Not applicable.

**Data Availability Statement:** Not applicable.

**Conflicts of Interest:** The authors declare no conflict of interest.

**Sample Availability:** Samples of the compounds are not available.

## References

1. Carroll, A.R.; Copp, B.R.; Davis, R.A.; Keyzers, R.A.; Prinsep, M.R. Marine natural products. *Nat. Prod. Rep.* **2022**, *39*, 1122–1171. [CrossRef] [PubMed]
2. Cheng, M.M.; Tang, X.L.; Sun, Y.T.; Song, D.Y.; Cheng, Y.J.; Liu, H.; Li, P.L.; Li, G.Q. Biological and chemical diversity of marine sponge-derived microorganisms over the last two decades from 1998 to 2017. *Molecules* **2020**, *25*, 853. [CrossRef] [PubMed]
3. Blunt, J.W.; Carroll, A.R.; Copp, B.R.; Davis, R.A.; Keyzers, R.A.; Prinsep, M.R. Marine natural products. *Nat. Prod. Rep.* **2018**, *35*, 8–53. [CrossRef] [PubMed]
4. Carroll, A.R.; Copp, B.R.; Davis, R.A.; Keyzers, R.A.; Prinsep, M.R. Marine natural products. *Nat. Prod. Rep.* **2019**, *36*, 122–173. [CrossRef] [PubMed]
5. Carroll, A.R.; Copp, B.R.; Davis, R.A.; Keyzers, R.A.; Prinsep, M.R. Marine natural products. *Nat. Prod. Rep.* **2020**, *37*, 175–223. [CrossRef] [PubMed]
6. Morita, M.; Schmidt, E.W. Parallel lives of symbionts and hosts: Chemical mutualism in marine animals. *Nat. Prod. Rep.* **2018**, *35*, 357–378. [CrossRef]
7. Bian, C.; Wang, J.; Zhou, X.; Wu, W.; Guo, R. Recent Advances on Marine Alkaloids from Sponges. *Chem. Biodivers.* **2020**, *17*, e2000186. [CrossRef]
8. Zhang, B.; Higuchi, R.; Miyamoto, T.; Soest, R.W.M.V. Neuritogenic Activity-Guided Isolation of a Free Base Form Manzamine A from a Marine Sponge, *Acanthostrongylophora* aff. *ingens* (Thiele, 1899). *Chem. Pharm. Bull.* **2008**, *56*, 866–869. [CrossRef]
9. Waters, A.L.; Peraud, O.; Kasanah, N.; Sims, J.W.; Kothalawala, N.; Anderson, M.A.; Abbas, S.H.; Rao, K.V.; Jupally, V.R.; Kelly, M.; et al. An analysis of the sponge *Acanthostrongylophora igens* microbiome yields an actinomycete that produces the natural product manzamine A. *Front. Mar. Sci.* **2014**, *1*, 54. [CrossRef]
10. McKay, M.J.; Carroll, A.R.; Quinn, R.J.; Hooper, J.N.A. 1, 2-Bis (1 H-indol-3-yl) ethane-1, 2-dione, an Indole Alkaloid from the Marine Sponge *Smenospongia* sp. *J. Nat. Prod.* **2002**, *65*, 595–597. [CrossRef]
11. Asiri, I.A.M.; Badr, J.M.; Youssef, D.T.A. Penicillivinacine, antimigratory diketopiperazine alkaloid from the marine-derived fungus *Penicillium vinaceum*. *Phytochem. Lett.* **2015**, *13*, 53–58. [CrossRef]
12. Granmo, A.; Petrini, L.E. A new species of Lopadostoma, and the anamorph of *Biscogniauxia cinereolilacina*. *Mycol. Helv.* **1996**, *8*, 43–50.
13. Jaklitsch, W.M.; Fournier, J.; Rogers, J.D.; Voglmayr, H. Phylogenetic and taxonomic revision of *Lopadostoma*. *Pers.-Mol. Phylogeny Evol. Fungi* **2014**, *32*, 52–82. [CrossRef] [PubMed]
14. Helaly, S.E.; Thongbai, B.; Stadler, M. Diversity of biologically active secondary metabolites from endophytic and saprotrophic fungi of the ascomycete order *Xylariales*. *Nat. Prod. Rep.* **2018**, *35*, 992–1014. [CrossRef] [PubMed]
15. Quang, D.N.; Hashimoto, T.; Fournier, J.; Stadler, M.; Radulović, N.; Asakawa, Y. Sassafrins A–D, new antimicrobial azaphilones from the fungus *Creosphaeria sassafras*. *Tetrahedron* **2005**, *61*, 1743–1748. [CrossRef]
16. Smetanina, O.F.; Yurchenko, A.N.; Ivanets, E.V.; Gerasimenko, A.V.; Trinh, P.T.H.; Ly, B.M.; Nhut, N.D.; Van, T.T.T.; Yurchenko, E.A.; Afiyatullov, S.S. Aromatic Metabolites of Marine Fungus *Penicillium* sp. KMM 4672 Associated with a Brown Alga *Padina* sp. *Chem. Nat. Compd.* **2017**, *53*, 600–602. [CrossRef]
17. Yurchenko, A.N.; Trinh, P.T.H.; Girich, E.V.; Smetanina, O.F.; Rasin, A.B.; Popov, R.S.; Dyshlovoy, S.A.; von Amsberg, G.; Menchinskaya, E.S.; Van, T.T.T.; et al. Biologically Active Metabolites from the Marine Sediment-Derived Fungus *Aspergillus flocculosus*. *Mar. Drugs* **2019**, *17*, 579. [CrossRef]
18. Kusumi, T.; Ooi, T.; Ohkubo, Y.; Yabuuchi, T. The modified Mosher's method and the sulfoximine method. *Bull. Chem. Soc. Jpn.* **2006**, *79*, 965–980. [CrossRef]

19. Xu, D.X.; Sun, P.; Kurtán, T.; Mándi, A.; Tang, H.; Liu, B.; Gerwick, W.H.; Wang, Z.W.; Zhang, W. Polyhydroxy cyclohexanols from a *Dendrodochium* sp. fungus associated with the sea cucumber holothuria *Nobilis selenka*. *J. Nat. Prod.* **2014**, *77*, 1179–1184. [CrossRef]
20. Grove, J.F. The structure of gliorosein. *J. Chem. Soc. C Org.* **1966**, 985. [CrossRef]
21. Shushni, M.A.M.; Singh, R.; Mentel, R.; Lindequist, U. Balticolid: A new 12-membered macrolide with antiviral activity from an Ascomycetous fungus of marine origin. *Mar. Drugs* **2011**, *9*, 844–851. [CrossRef] [PubMed]
22. Sun, P.; Xu, D.X.; Mándi, A.; Kurtán, T.; Li, T.J.; Schulz, B.; Zhang, W. Structure, absolute configuration, and conformational study of 12-membered macrolides from the fungus dendrodochium sp. associated with the sea cucumber holothuria nobilis selenka. *J. Org. Chem.* **2013**, *78*, 7030–7047. [CrossRef] [PubMed]
23. Kokubun, T.; Veitch, N.C.; Bridge, P.D.; Simmonds, M.S.J. Dihydroisocoumarins and a tetralone from Cytospora eucalypticola. *Phytochemistry* **2003**, *62*, 779–782. [CrossRef]
24. Arora, D.; Sharma, N.; Singamaneni, V.; Sharma, V.; Kushwaha, M.; Abrol, V.; Guru, S.; Sharma, S.; Gupta, A.P.; Bhushan, S.; et al. Isolation and characterization of bioactive metabolites from Xylaria psidii, an endophytic fungus of the medicinal plant Aegle marmelos and their role in mitochondrial dependent apoptosis against pancreatic cancer cells. *Phytomedicine* **2016**, *23*, 1312–1320. [CrossRef] [PubMed]
25. Brian, P.W.; Curtis, P.J.; Howland, S.R.; Jefferys, E.G.; Raudnitz, H. Three new antibiotics from a species of *Gliocladium*. *Experientia* **1951**, *7*, 266–267. [CrossRef]
26. Steward, M.W.; Packter, N.M. Incorporation of 5-methylorcylaldehyde and methionine into the acetogenin (polyketide) gliorosein in Gliocladium roseum IMI. 93065. *Biochem. J.* **1968**, *109*, 1–11. [CrossRef]
27. Vischer, E.B. The structures of aurantio- and rubro-gliocladin and gliorosein. *J. Chem. Soc.* **1953**, 815–820. [CrossRef]
28. Muñoz-Sánchez, J.; Chánez-Cárdenas, M.E. The use of cobalt chloride as a chemical hypoxia model. *J. Appl. Toxicol.* **2019**, *39*, 556–570. [CrossRef]
29. Chen, R.; Lai, U.H.; Zhu, L.; Singh, A.; Ahmed, M.; Forsyth, N.R. Reactive oxygen species formation in the brain at different oxygen levels: The role of hypoxia inducible factors. *Front. Cell Dev. Biol.* **2018**, *6*, 132. [CrossRef]
30. Li, M.; Li, K.; Ren, Y. Nesfatin-1 protects H9c2 cardiomyocytes against cobalt chloride-induced hypoxic injury by modulating the MAPK and Notch1 signaling pathways. *J. Biol. Res. Thessalon.* **2021**, *28*, 21. [CrossRef]
31. Segura-Aguilar, J. Neurotoxins as Preclinical Models for Parkinson's Disease. *Neurotox. Res.* **2018**, *34*, 870–877. [CrossRef] [PubMed]
32. Liang, S.; Figtree, G.; Aiqun, M.; Ping, Z. GAPDH-knockdown reduce rotenone-induced H9C2 cells death via autophagy and anti-oxidative stress pathway. *Toxicol. Lett.* **2015**, *234*, 162–171. [CrossRef] [PubMed]
33. Yaakoub, H.; Mina, S.; Calenda, A.; Bouchara, J.P.; Papon, N. Oxidative stress response pathways in fungi. *Cell. Mol. Life Sci.* **2022**, *79*, 333. [CrossRef]
34. Yurchenko, E.A.; Menchinskaya, E.S.; Pislyagin, E.A.; Trinh, P.T.H.; Ivanets, E.V.; Smetanina, O.F.; Yurchenko, A.N. Neuroprotective Activity of Some Marine Fungal Metabolites in the 6-Hydroxydopamin- and Paraquat-Induced Parkinson's Disease Models. *Mar. Drugs* **2018**, *16*, 457. [CrossRef] [PubMed]